Al-Qadisiyah Journal of Pure Science Vol. (31) Issue (Special) (2026) pp. 396– 410

Al-Qadisiyah Journal of Pure Science

ISSN(Printed): 1997-2490 ISSN(Online): 2411-3514

DOI: 10.29350/jops

Al-Qadisiyah Journal of Pure Science

Fluorescent Biosensor for the Detection of Biological Analytes in Aqueous Solutions

Haneen Ghanem Bahloul[1], Bassam Faroun Abdul Farhani[2]

Received: 14/05/2026; Accepted: 17/05/2026.

ABSTRACT

An easy and cost-effective technique was adopted to synthesize tannic acid-capped AgNPs and to develop a fluorescent silver sensor system to detect ferric ion (Fe^{3+}) in water. The AgNPs were characterized using UV-Vis absorption, FTIR, EDX, and XRD. The AgNPs in this study were strongly fluorescent with an excitation and emission maximum of 363 and 444 nm, respectively. Fluorescence of nanoparticles was quenched in the existence of Fe^{3+}ions relative to other metal ions, thus indicating a good selectivity of the nanoparticles for ferric ions. A linear regression was obtained with a correlation coefficient (R^2) of 0.995 for concentrations ranging between 50-250 µM of Fe^{3+}. The limit of detection (LOD) was 0.207968 µM. The findings show that AgNPs capped with tannic acid can be used as a simple, sensitive, and selective fluorescent probe for the detection of Fe^{3+} ions in water.

Introduction

The increasing need for fast and reliable analytical methods in last few periods has triggered the quick improvement of point-of-care testing (POCT) devices. These systems have received significant attention for their many applications in environmental, medical, and food analysis, where real-time detection on-site is essential [1], [2]. As a result, the development

of portable, easy-to-operate, and affordable analytical systems has attracted great attention in the modern analytical field.

Among the new techniques, paper-based analytical devices (PADs) have gained considerable attention for on-site analysis. The integration of microfluidic technologies and the enhancement of fluorescence on the substrate have led to the development of paper-based devices with enhanced analytical performance in terms of sensitivity, allowing highly sensitive detection of various contaminants in environmental and food samples while ensuring simplicity and low cost of production [3], [4].

Among the materials, noble metal nanomaterials (NMNs), such as nanoparticles of Ag, Au, Cu, Pt, and Pd, have received growing attention for the development of POCT devices. The unique optical characteristics of these nanomaterials, especially surface plasmon resonance (SPR), have allowed the creation of highly sensitive and efficient colorimetric sensors that are simple, sensitive, and inexpensive [5], [6].

In particular, AgNPs are one of the most promising noble metal nanostructures because of their intense plasmonic absorption bands, yellow color, high stability, and high conductivity. These unique physicochemical characteristics have made them generally utilized in a variety of uses for example food preservation technologies, sensors, and textiles [7], [8].

However, traditional spectroscopic detection approaches using AgNPs typically require laboratory-synthesized nanoparticles, expensive equipment, and highly trained personnel to operate. This may limit their potential in real-time monitoring and on-site detection. Recently, a new approach has been put forward involving controlled dispersion and immobilization of AgNPs on solid supports, which provides an attractive avenue for improvement of simple and user-friendly POCT platforms for convenient naked-eye detection systems [9]. Tannic acid (TA) is a water-soluble polyphenol found in plants, fruit peels, and beverages [10]. The U.S. Food and Drug Administration (FDA) has approved tannic acid as a safe substance, and it can be directly applied in drug research [11]. Tannic

acid molecules have a rich phenolic hydroxyl functional group structure that can interact with metal ions and nanomaterial surfaces. These groups allow tannic acid to serve as a reducing and capping agent for the preparation of metal nanoparticles. These distinctive chemical properties of tannic acid make it a promising decreasing agent for synthesis of nanomaterials and sensing applications.

Given these factors, our current research is directed towards the preparation of silver nanoparticles utilizing tannic acid as a decreasing and stabilizing agent. The new synthesized AgNPs were tested as a fluorescent sensor in existence of metal ions. The detection mechanism was evaluated by determining the fluorescence emission in the existence of various metal salts. We observed that Fe^{3+} ions, particularly those from iron (III) chloride hexahydrate, were the most effective in quenching the fluorescence. This technique demonstrates the potential of tannic acid-capped AgNPs as a tool for easy and sensitive sensing of metal ions.

Experimental

Materials

Silver nitrate ($AgNO_3$, 99%), tannic acid (98%), NaOH, 98%, iron(III) chloride hexahydrate ($FeCl_3 \cdot 6H_2O$, 98%), trisodium citrate ($Na_3C_6H_5O_7$, 99%), and mercury(II) nitrate ($Hg(NO_3)_2$, 99%) were obtained from Sigma-Aldrich, while potassium chloride (KCl, 99%), calcium chloride ($CaCl_2$, 99%), lead(II) nitrate ($Pb(NO_3)_2$, 99%), magnesium nitrate ($Mg(NO_3)_2$, 99%), and zinc acetate ($Zn(CH_3COO)_2$, 99%) were obtained from BDH. Chromium (III) chloride hexahydrate ($CrCl_3 \cdot 6H_2O$, 98%) and iron (II) chloride tetrahydrate ($FeCl_2 \cdot 4H_2O$, 98%) were obtained from Sigma. Distilled water (H_2O) was supplied by the laboratory and used as received without further purification.

Instrumentation

The pH meter (inoLab pH 7110 SET 2, WTW, Germany) and the hot plate stirrer (UC 152, Stuart, UK) were used in this study. The RF-5301PC spectrofluorophotometer (Shimadzu, Japan) was used for fluorescence measurements, and the UV-1800 UV–visible spectrophotometer (Shimadzu, Japan) was utilized to measure the UV–vis absorption spectra.

The ATR- FTIR spectrophotometer (Tensor 27, Bruker, Germany) was utilized to detect functional collections. The morphology of surface was studied using the FE-SEM, Thermo Fisher Scientific, Netherlands). The X-ray diffractometer (XRD, Aeris benchtop, Malvern Panalytical, Netherlands) was utilized for the crystallinity test.

An electronic balance (BL 210S, ±0.0001 g, Sartorius, Germany) was used for weighing, and an oven (LDO-060E, Labtech, Korea) was used for drying.

Preparation of TA-AgNPs

The chemical reduction method was used to prepare AgNPs utlizing tannic acid as a decreasing and stabilising agent. Typically, 30 µL of 2 M silver nitrate ($AgNO_3$) solution was additional to 50 mL of distilled water with constant stirring, and solution was brought to a boil on a hot plate stirrer.

Once the solution was boiling, 2 mL of 2% (w/v) tannic acid solution was added dropwise under constant stirring. The reaction mixture was then made strongly alkaline (pH 11-12) using sodium hydroxide (NaOH) solution to promote the reduction of silver ions. The solution was maintained at the boiling point for 10 min, and the color of the solution started to change to dark brown during this period, indicating the formation of silver nanoparticles due to surface plasmon resonance (SPR).

The response mix was then cooled to room temperatures, and nanoparticles obtained were isolated by centrifugation at 10,000 rpm for 20 min to take out by-products. The precipitate was washed and then re-dispersed in distilled water to prepare a stable colloidal suspension of TA-AgNPs for further analysis and applications.

In this approach, tannic acid acts as a decreasing agent by decreasing Ag^{+} to Ag^{0} and as a capping agent by binding its phenolic groups to the surface of the nanoparticles to prevent aggregation and enhance the stability of the nanoparticles.

Detection Procedure for Fe (III) Ions in Aqueous Medium

A stock standard solution of Fe (III) ions (0.06 M) was carried out by accurately weighing ferric chloride hexahydrate ($FeCl_3 \cdot 6H_2O$) and dissolving it in deionized distilled water, followed by diluting to 100 mL in a volumetric flask. Then, a series of Fe (III) solutions of varying concentrations was carried out by serial dilution. For analytical purposes, Fe (III) solutions (50-250 µM) were carried out by volumetric dilution of stock solution. These were used for the nanoparticles detection and for building the calibration curve. For the detection, a constant quantity of TA-AgNPs was added to the fluorescence cell, and different concentrations of the Fe (III) ion solutions. After thorough mixing, the change in fluorescence intensity resulting from the relations between Fe (III) ions and functional groups present on nanoparticle surface was recorded. Fluorescence measurements were carried out using a fluorescence spectrophotometer at suitable excitation and emission wavelengths. The variations in fluorescence intensity were used to evaluate the sensitivity and selectivity of the sensing system toward Fe (III) ions. All measurements were performed at room temperature.

3. Results and Discussion

3.1. Morphological analysis and characterization

XRD Analysis of Silver Nanoparticles

XRD form of synthesized silver nanoparticles was recorded using a PANalytical Aeris X-ray diffractometer with Cu-Kα radiation having a wavelength of 0.15406 nm. The measurements were carried out at a working voltage of 40 kV and a existing of 7.5 mA. A nickel (Ni) filter was used to remove Cu-Kβ radiation. The diffraction data were together over a 2θ range with a scanning stage size of 0.02°.

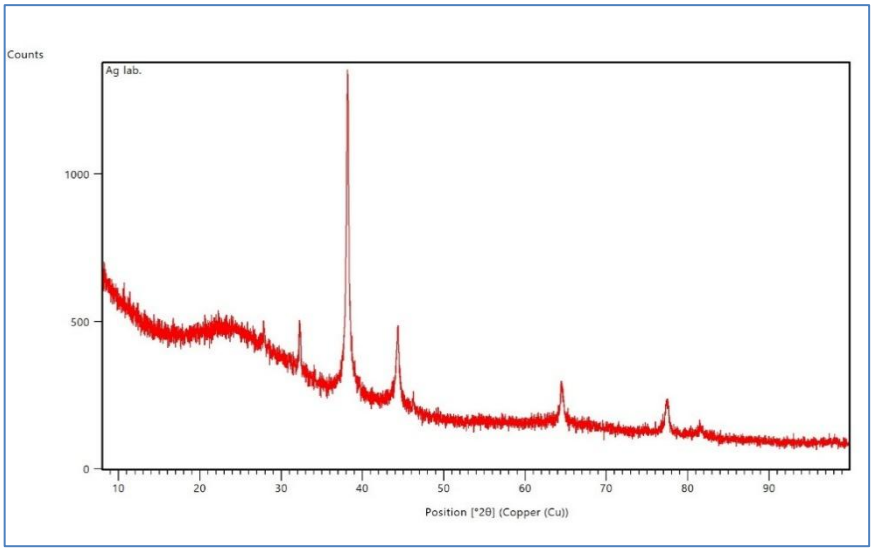

Figure (3-1): XRD form of synthesized AgNPs recorded utilizing Cu–Kα radiation.

The XRD form of the synthesized silver nanoparticles is presented in Figure (3-1). Distinct diffraction peaks were experiential at approximately 38.10°, 44.30°, 64.50°, and 77.40°, that correspond to crystallographic planes (111), (200), (220), and (311), respectively. The positions of these peaks are in decent agreement with standard silver data file (JCPDS card No. 96-500-0219), confirming that the synthesized nanoparticles possess a FCC crystal construction. [12,13]

The most intense diffraction peak appeared at 2θ ≈ 38.10°, conforming to the (111) plane, which is considered the most stable crystallographic plane in the silver lattice [14,12,15,16,17,18]. The XRD form shows that there are no extra peaks, which suggests that the nanoparticles have good phase purity and that there are no other crystalline phases and/or impurities, which is an indication of successful preparation of silver nanoparticles.

The interplanar spacing (d-spacing) was determined with the help of Bragg's law, as shown in the equation: [19]

$d=n\lambda/(2\sin\theta)$

where d is interplanar distance, n is an integer, λ is wavelength of the X-ray, and θ is diffraction angle.

The crystallite size of the nanoparticles was determined utilizing Debye–Scherrer formula: [19]

$D=k\lambda/(\beta \cos\theta)$

In which D is average crystallite size, k is shape factor, λ is the X-ray wavelength, β is the FWHM of diffraction peak, and θ is the Bragg diffraction angle.

2θ (deg)	FWHM	Crystal Size (nm)	Intensity	d-spacing (Å)	Miller index
38.10	0.32	30.6	1334	2.36	(111)
44.30	0.41	25.3	1105	2.04	(200)
64.50	0.52	20.7	872	1.44	(220)
77.40	0.60	18.0	640	1.23	(311)

Table (3-1) shows the diffraction angles, peak intensities, full widths at half maximum (FWHM), d-spacing, and the calculated crystallite size of prepared silver nanoparticles.

Table (3-1) shows that crystallite size of nanoparticles ranges from 18 to 30 nm, with an average of around 23 nm, indicating that the nanoparticles are indeed in the nanoscale range.

These outcomes are in agreement with some of the previous reports of diffraction peaks of silver nanoparticles at nearly 38°, 44°, 64°, and 77° due to the (111), (200), (220), and (311) of the FCC construction of silver. The narrow width and strong intensity of the diffraction peaks reveal that the nanoparticles have a great crystallinity and good crystalline structure.

Thus, the XRD findings confirm the synthesis of silver nanoparticles with a good crystalline construction and a nanometer-range crystallite size.

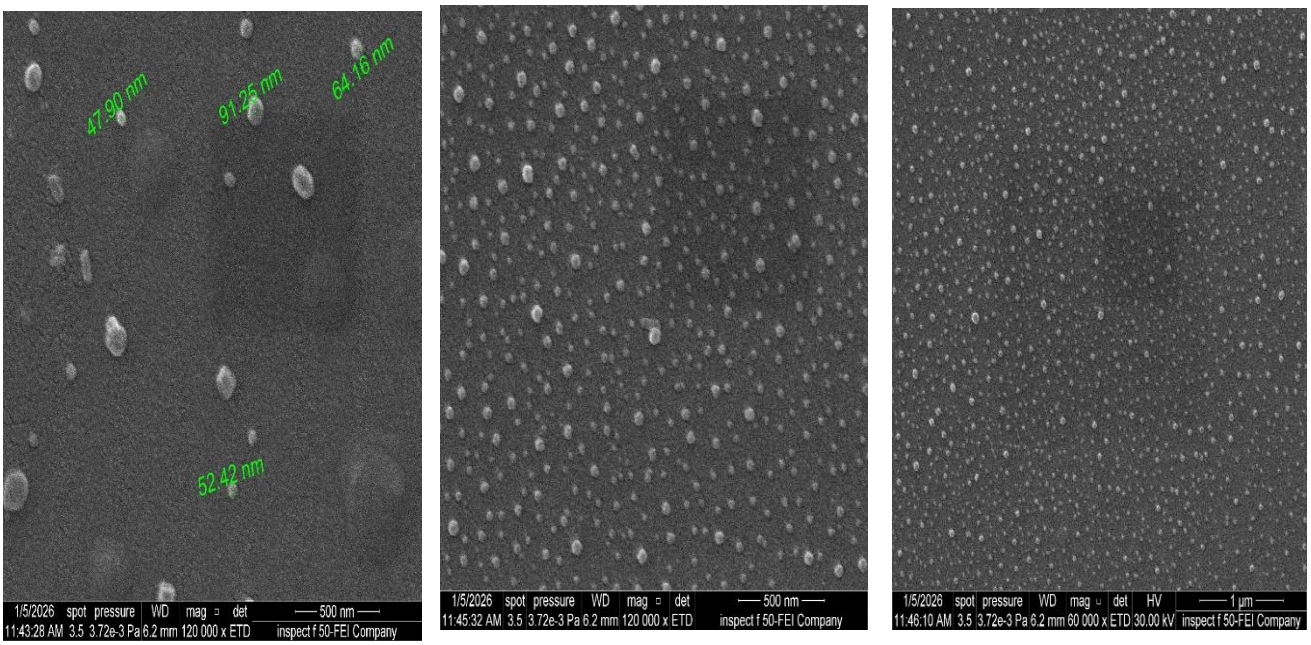

Fig. (3-2). SEM images of silver nanoparticles (AgNPs): (a) SEM image showing the estimated sizes of the particles, (b,c) SEM pictures display shape and uniform distribution of AgNPs.

FT-IR Spectral Analysis

FT-IR spectrum of TA capped AgNPs in the range 4000-500 cm^{-1} is shown in Figure (3-5). The FT-IR study was conducted to determine functional collections that are accountable for decrease of silver ions and stabilization of synthesized nanoparticles.

The spectrum shows a broad absorption band in range of 3746-3436 cm-1, which is associated with the stretching vibrations of the hydroxyl (O-H) collections of the phenolic collections of tannic acid molecules. These groups have been reported to be contained in decline of Ag^{+} ions to metallic silver (Ag^{0}) during the synthesis.

A prominent absorption band around 3125 cm^{-1} is due to the aromatic C-H stretching vibration, suggesting the presence of aromatic rings from tannic acid molecules bound to nanoparticle surface. Furthermore, the bands in the range 2920-2840 cm^{-1} are attributed to

aliphatic C-H stretching vibrations, which may show existence of organic byproducts around nanoparticles.

Moreover, the absorption band observed around 1701 cm^{-1} corresponds to stretching vibrations of carbonyl (C=O) group, which may be because of the presence of oxidized phenolic collections or quinone structures resulting from the reduction of tannic acid. The absorption band around 1600-1500 cm^{-1} is attributed to stretching vibration of the C=C collection of aromatic rings, which is indicative of existence of polyphenolic mixes in tannic acid.

Additionally, band at 1344 cm^{-1} corresponds to stretching vibration of the carboxylate (COO^{-}) collection, and is indicative of the interaction between tannic acid molecules and the surface of silver nanoparticles. The bands experiential at 1180-1040 cm^{-1} are because of the C-O stretching vibrations, which are prominent in phenolic and alcoholic groups of tannic acid.

Several other peaks are present in fingerprint area (1000-500 $cm^{-}1$), which are because of out-of-plane deformation of aromatic C-H bonds and other vibrations of the organic molecules attached to the nanoparticle surface.

The findings clearly demonstrate the role of tannic acid as a decreasing and a capping agent in formation of (AgNPs). These hydroxyl, carbonyl, and carboxylate groups play a part in decline of silver ions, and also help in stabilization of nanoparticles by preventing aggregation and confirming the successful synthesis of tannic acid-capped silver nanoparticles (AgNPs). [20,21,22]

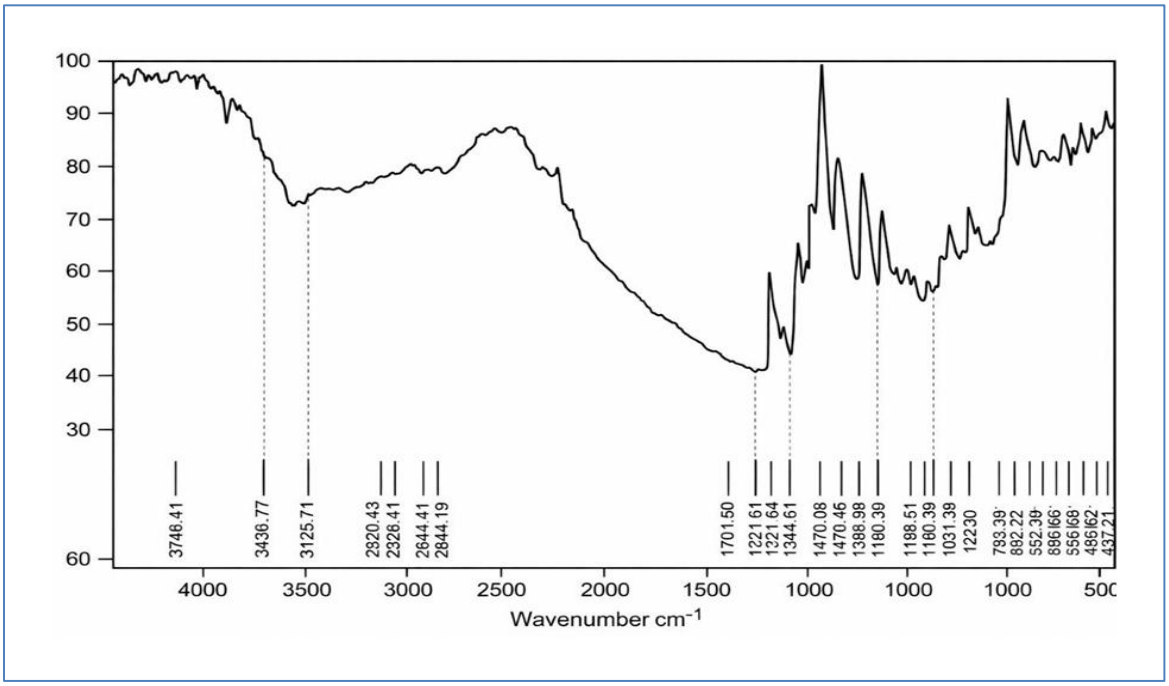

Figure (3-5): FT-IR spectrum of the prepared AgNP).

The elemental analysis of silver nanoparticles was carried out by EDX. In the figure, the EDX spectrum shows a strong peak at the element silver (Ag), which confirms that silver is the main element present in the nanoparticles. Furthermore, small peaks of other elements, including O, Na, Mg, and Ca were also detected. These elements could be remnants of compounds used in the synthesis process or from the sample holder itself.

The presence of the silver peak in the EDX spectrum indicates the successful preparation of silver nanoparticles (AgNPs)

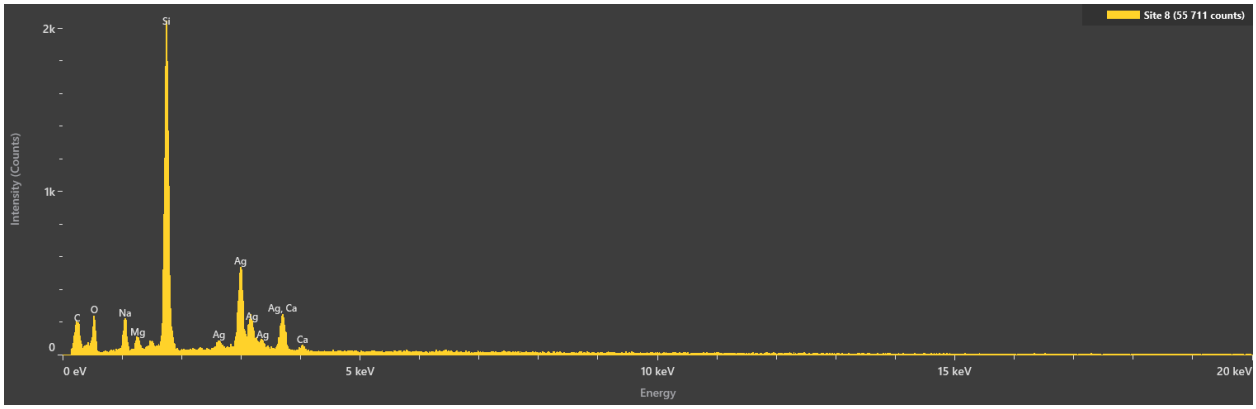

Figure (3-6): EDX spectrum of AgNPs reveals silver (Ag) as the major element present in the sample.

The UV-Visible absorption spectrum of silver nanoparticles has been recorded utilizing UV-Vis spectrophotometer in the range of 200-700 nm and are given in Figure 5-7 A strong and narrow absorption peak is seen in the visible area (at approximately 400 nm) corresponding to LSPR effect of silver nanoparticles. This is due to collective oscillations of allowed electrons on the surface of nanoparticles in the existence of an electromagnetic field, which results in absorption of light at a specific wavelength. This indicates the existence of silver nanoparticles in the solution. In addition, the peak position is very sensitive to other factors such as the size, form, size-distribution of the nanoparticles and the refractive index of the medium. The observed peak at approximately 400 nm suggests the formation of relatively small-sized silver nanoparticles with a fairly uniform size distribution, as the absorption peaks of silver nanoparticles typically appear within the range of 380–450 nm.In addition, a gradual reduction in absorbance amount is experiential at wavelengths higher than peak region. This decrease can be attributed to the reduced plasmon resonance effect outside the resonance region, in addition to the light scattering effect caused by the nanoparticles. These results indicate the formation of stable silver nanoparticles with distinctive optical properties, which are consistent with numerous previously reported studies in scientific literature on metallic nanoparticles.

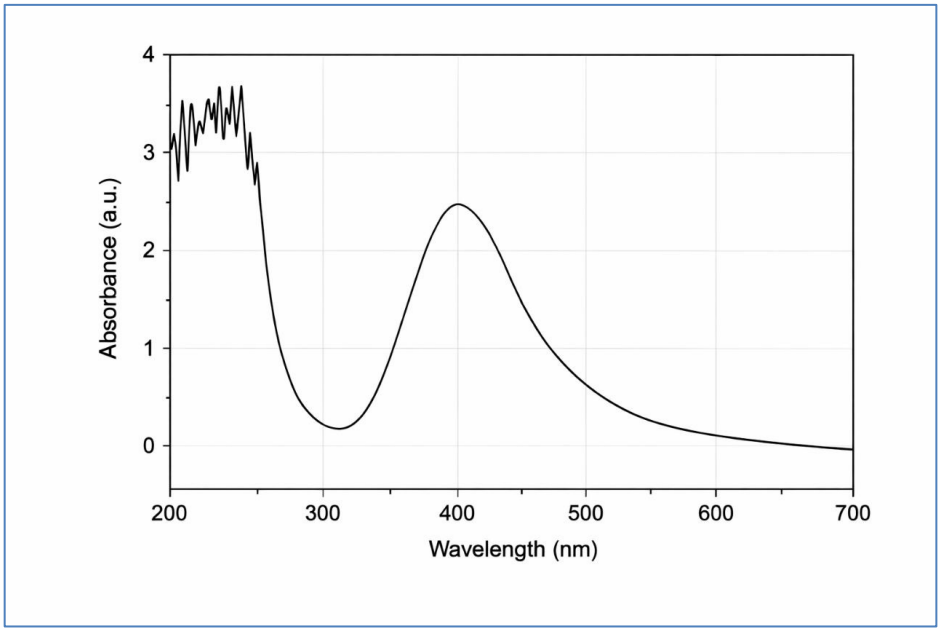

Figure (5-7): UV–Visible (UV–Vis) absorption spectrum of synthesized AgNPs.

Conclusion

In this research, tannic acid-capped silver nanoparticles (AgNPs) were positively synthesized utilizing a simple and cost-effective technique. The as-synthesized nanoparticles have excellent fluorescent characteristics with an excitation peak at 363 nm and an emission peak at 444 nm. The synthesised AgNPs showed a strong selectivity towards Fe^{3+} ions compared to other metal ions, and they were fluorescence quenchers. A linear response was observed amid fluorescence intensity and Fe^{3+} concentration in range of 50-250 µM. The fluorescent sensor also showed good sensitivity in artificial urine, and it can be used for Fe^{3+} ions measurements in biological samples. So, tannic acid-functionalised AgNPs are a good fluorescent sensor for selective and sensitive revealing of Fe^{3+} ions in water and biological media.

Reference

W. Qiu et al., Auto-fluorescence of cellulose paper with partial nitric phase dispersion-induced fluorescence enhancement behavior for three heavy metal ions detection, Food Chemistry, 2020.

M. Maruthupandi et al Ultrasensitive and selective detection of cadmium ions in hair, nail, cigarette and wastewater samples using disulfo-stilbenediamine capped silver nanoparticles J Mol Struct (2022).

M. Maruthupandi et al., One minute synthesis of green fluorescent copper nanocluster: the preparation of smartphone aided paper-based kit for on-site monitoring of nanomolar level mercury and sulfide ions in environmental samples, Journal of Hazardous Materials, 2020.

D. L. A. Fernandes et al., A new analytical system, based on an acoustic wave sensor, for halitosis evaluation, Sensors and Actuators B: Chemical, 2009.

D. Tang et al., Sensitive determination of dissolved sulfide in estuarine water by solid-phase extraction and high-performance liquid chromatography of methylene blue, Journal of Chromatography A, 2000.

X. Dighi et al., Electrocatalytic oxidation of sulphide using a pencil graphite electrode modified with hematoxylin, Sensors and Actuators B: Chemical, 2022.

M. Sun et al., Two-dimensional p-n heterojunctions of black phosphorus nanosheet-sensitized α-MoO3 nanoflake for low-temperature chemiresistive NH3 recognition, Microchemical Journal, 2022.

A. E. Bretthall et al., Validation of analytical test methods, Separation Science and Technology, 2011.

Mercy, J. S. I.; Vasimalai, N. Point-of-care sensor kit for on-site monitoring of creatinine in clinical samples using polyol functionalized gold nanoparticles by UV–visible spectrophotometry. Microchemical Journal 2023, 193, 109173.

Li, N., et al. (2018). Adenosine-derived doped carbon dots: From an insight into the effect of N/P co-doping on emission to highly sensitive picric acid sensing. Analytica Chimica Acta, 1028, 17–26.

Yi, S., et al. (2020). Amphiphilic gemini-iridium (III) complex for rapid and selective detection of picric acid in water and intracellular environments. Talanta, 208, 120387.

Yi, Z.; Li, X.; Xu, X.; Luo, B.; Luo, J.; Wu, W.; Yi, Y.; Tang, Y. Green, effective chemical route for the synthesis of silver nanoplates in tannic acid aqueous solution. Colloids Surf., A 2011

Chouhan, N.; Ameta, R.; Meena, R. K. Biogenic silver nanoparticles from Trachyspermum ammi (Ajwain) seeds extract for catalytic reduction of p-nitrophenol to p-aminophenol in excess of NaBH4. J. Mol. Liq. 2017

R, V. K. R.; K, V. A.; P S, K.; Singh, S. P. Conductive silver inks and their applications in printed and flexible electronics. RSC Adv. 2015

Hao, Y.; Zhang, N.; Luo, J.; Liu, X. Green Synthesis of Silver Nanoparticles by Tannic Acid with Improved Catalytic Performance Towards the Reduction of Methylene Blue. Nano 2017

Karuppannan, K.; Nagaraj, E.; Sujatha, V. Green Synthesis and Biological Applications of Silver Nanoparticles Using Phyllanthus maderaspatensis L. Root Extract. Smart Sci. 2016

Kim, T. Y.; Cha, S.-H.; Cho, S.; Park, Y. Tannic acid-mediated green synthesis of antibacterial silver nanoparticles. Arch. Pharmacal Res. 2016

Mamidi, G.; Polaki, S. J. A. C. Synthesis and Characterization of Biogenic Silver Nanoparticles and its Antimicrobial Analysis. J. Appl. Chem. 2019

Moon, K.-S.; Dong, H.; Maric, R.; Pothukuchi, S.; Hunt, A.; Li, Y.; Wong, C. P. Thermal behavior of silver nanoparticles for low-temperature interconnect applications. J. Electron. Mater. 2005

Hao, Y.; Zhang, N.; Luo, J.; Liu, X. Green Synthesis of Silver Nanoparticles by Tannic Acid with Improved Catalytic Performance Towards the Reduction of Methylene Blue. Nano 2017,

Ranoszek-Soliwoda, K.; Tomaszewska, E.; Socha, E.; Krzyczmonik, P.; Ignaczak, A.; Orlowski, P.; Krzyzowska, M.; Celichowski, G.; Grobelny, J. The role of tannic acid and sodium citrate in the synthesis of silver nanoparticles. J. Nanopart. Res. 2017

Socrates, G. Infrared and Raman Characteristic Group Frequencies: Tables and Charts, 3rd ed.; John Wiley & Sons, 2004.